Energy loss of protons in W using fully relativistic calculations and mean excitation energies of W, Au, Pb, and Bi

C. C. Montanari,[*] D. M. Mitnik, C. D. Archubi, and J. E. Miraglia

Instituto de Astronomía y Física del Espacio, Casilla de Correo 67, Sucursal 28, C1428EGA Buenos Aires, Argentina
and Departamento de Física, Facultad de Ciencias Exactas y Naturales, Universidad de Buenos Aires, Pabellón I,
Ciudad Universitaria, C1428EGA Buenos Aires, Argentina

We present a theoretical study on the energy loss of protons in wolframium by calculating target fully relativistic wave functions and binding energies. The HULLAC code is employed to obtain numerical solutions of the Dirac equation. We use the shellwise local plasma approximation (SLPA) to evaluate the different moments of the energy loss. The partial contribution of each subshell of target electrons is calculated separately, including the screening among the electrons of the same binding energy. We pay special attention to the role of the outer $4f$ shell and the screening between electrons of near subshells (i.e., the $5p$ and $4f$ electrons). Results for stopping and straggling cross sections are compared to the experimental data available. Our calculations describe rather well the stopping measurements around the maximum and for very high energies, but overestimate the data for impact energies around 1MeV. We find that the SLPA results tend clearly to Bethe limit, but show a systematic overestimation in the energy region of 1–2 MeV. This overestimation may indicate the presence of other mechanisms included neither in the SLPA nor in Bethe formulations. We also present results for the stopping number of W, Au, Pb, and Bi which follow quite well the Lindhard scaling. A theoretical mean excitation energy $I(W) = 710$ eV is obtained, in good agreement with the suggested value of 727 ± 30 eV. Theoretical mean excitation energies for Au, Pb, and Bi are also presented, which are in good agreement with the experimental ones.

PACS number(s): 34.50.Bw

I. INTRODUCTION

The study of the energy loss by ions in solids is a powerful tool on many areas of basic science and material technology [1–3]. Semiempirical tables and codes are extensively tested and used and they are freely available in the web [4,5] for a large combination of ions and targets.

On the other hand, multielectronic atoms are a heavy task for first-principles theories. There are detailed models to describe the response of outer electrons as a free-electron gas (FEG) [6–8]. In the low- or even intermediate-energy region, this contribution is the main one. But for targets with full d or f shells, the bound-electron contribution plays an important role even at energies around 10–20 keV. The theoretical description of inner (or bound) electrons of these targets is not so abundant (see, for example, the binary collisional formalism in Refs. [9,10] or the dielectric formalism in Refs. [11,12]).

The aim of this work is to present *ab initio* calculations of the energy loss of protons in wolframium (W, atomic number $Z = 74$ and gas form [Xe] $4f^{14}5d^46s^2$). This metal is also known as tungsten, though for historical reasons related to its discovery, wolframium is the correct name [13].

It fulfills a double interest in basic and applied physics. In W, the $5d$ and $6s$ electrons respond to the FEG description, so the $4f$ subshell, with its 14 electrons, is the outer shell of bound electrons. This fact makes wolframium an interesting test for the atomic description and the study of possible collective effects. On the other hand, new interest has arisen due

to the construction of the international thermonuclear experimental reactor (ITER) in Caradache, France [14]. ITER is expected to demonstrate the scientific and technological feasibility of fusion energy for peaceful purposes by nominal operation of 500 MW fusion power for 400 s [15]. Still an issue for the fusion reactor is the choice of materials for plasma-facing components. Originally a mix of beryllium, graphite, and wolframium has been planned for ITER inner wall. But reactor studies foresee a full wolframium inner wall to ensure a sufficient lifetime of first wall components [16,17]. Atoms from that wall reach the plasma and atomic data are needed for plasma diagnostic purposes as well as for modeling.

The theoretical model employed is the shellwise local plasma approximation (SLPA). This is based on the local plasma approximation (LPA) [18–20] to deal with bound electrons as an inhomogeneous free-electron gas. We apply the LPA in its formulation within the dielectric formalism [21–23] but assuming independent shell approximation [12,24,25]. The binding energies (or ionization gaps) are also included explicitly by employing the Levine and Louie dielectric function [26].

SLPA allows us to calculate the different moments of the energy loss by the ion when at least one of the bound electrons is ionized. This is an *ab initio* calculation—no parameter is included, as far as bound electrons are considered—whose only inputs are the atomic densities of the different subshells and the corresponding binding energies. This many-electron model is especially suitable for the description of shells precisely like the $4f$, for which the shielding effects are expected to be important.

As we deal with atoms of large atomic number ($Z > 54$), we resort to solve numerically the Dirac equation. For this

_____
[*]mclaudia@iafe.uba.ar

TABLE I. Fully relativistic binding energies, E^{th}, and mean radius, $\langle r \rangle$, of neutral wolframium. Theoretical values are calculated with the HULLAC code [27,28]. Also included are the experimental values, E^{expt}, compiled by Williams [32]. The binding energies are in Rydbergs and the radius in atomic units. Note that the theoretical results correspond to an isolated atom while the experimental values are measured in the solid phase.

nlj	E^{expt}	E^{th}	$\langle r \rangle$
$1s$	5110.3	5114.2	0.0183
$2s$	889.38	878.89	0.0770
$2p-$	848.51	839.68	0.0637
$2p+$	750.24	739.86	0.0717
$3s$	207.30	202.90	0.201
$3p-$	189.30	185.80	0.190
$3p+$	167.7	164.1	0.205
$3d-$	137.6	135.3	0.180
$3d+$	133.0	130.6	0.184
$4s$	43.67	41.70	0.450
$4p-$	36.05	34.63	0.455
$4p+$	31.13	29.60	0.489
$4d-$	18.81	17.97	0.507
$4d+$	17.90	17.06	0.518
$5s$	5.56	5.89	1.06
$5p-$	3.33	3.75	1.16
$5p+$	2.70	2.98	1.26
$4f-$	2.46	2.59	0.602
$4f+$	2.31	2.42	0.612
$6s$		0.452	3.63
$5d-$		0.312	2.28
$5d+$		0.263	2.55

purpose, the HULLAC computer package [27,28] was employed. This combination of the fully relativistic calculation of binding energies and densities and the SLPA has been recently applied to collisions of protons with Au, Pb, and Bi [12]. The present work continues [12] and intends to get a deeper understanding of the asymptotic behavior of the SLPA.

In what follows, we present our theoretical formalism and results for the first (stopping) and second (straggling) moments of the energy loss. We also study the high-energy behavior of the SLPA and compare it to Bethe asymptotic stopping and with the recommended values of mean excitation energy [29]. This comparison is applied not only to W but also to Au, Pb, and Bi in a single plot using the scaling by Lindhard and Scharff [30].

We have organized this work in three steps. First, we describe the fully relativistic calculation and present results for atomic binding energies of W in comparison to experimental values and semirelativistic approaches. Second, the SLPA is described taking into account new considerations that apply to multielectronic targets. Finally, we present stopping and straggling cross sections together with mean excitation energies and compare our *ab initio* theoretical values to the experimental data available [5,29] and with the semiempirical
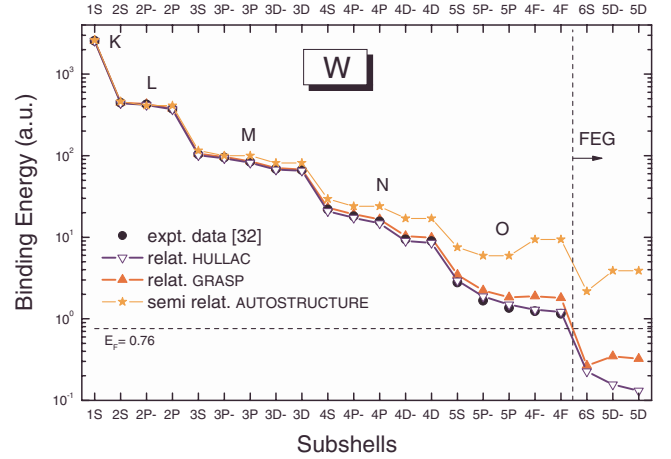
FIG. 1. (Color online) Electronic binding energies of W. Symbols: results of the relativistic HULLAC (down-hollow triangles), relativistic GRASP (up-filled triangles), and semirelativistic AUTOSTRUCTURE (stars) calculations; filled circles, experimental data in solids [32]. The Fermi energy E_F and the FEG subshells are indicated with dashed lines.

SRIM08 results [4]. Atomic units are used unless otherwise stated.

II. BINDING ENERGIES AND DENSITIES

We employed the HULLAC code [27,28] to solve numerically the Dirac equation, including the Breit interaction energies and quantum electrodynamic corrections in first-order perturbation theory. The detailed level energies are calculated using the fully relativistic multiconfigurational RELAC code [31]. A more detailed explanation of the procedure can be found in Ref. [12].

The HULLAC results for the binding energies of W are displayed in Table I together with the experimental values compiled by Williams [32]. The relativistic binding energies show the spin-orbit split $E_{n,l,l\pm1/2}$ (hereafter $nl\pm$). The agreement between theoretical (isolated atom) and experimental (in solid) energies is good, with the difference being less than 5%, except for the $5p\pm$ energies that is 10%. We also include in Table I the mean radius $\langle r \rangle_{nl\pm}$ of each subshell obtained by the integration of the fully relativistic radial functions.

In Fig. 1, we show a rather complete study of wolframium binding energies by comparing the HULLAC results to other semirelativistic and fully relativistic calculations. We also included in Fig. 1 the experimental results [32] for solid wolframium and the value of the Fermi energy for the FEG (basically the $5d^4$ and $6s^2$ electrons).

The semirelativistic binding energies were obtained using the AUTOSTRUCTURE code [33,34] with the radial wave functions evaluated with Slater-type orbitals. As these results have no spin-orbit split in energy, in Fig. 1, we plot each value twice just to make the comparison easier.

An alternative fully relativistic calculation was also performed by using the GRASP code [35,36]. As can be observed in Fig. 1, the GRASP results failed by little to describe the
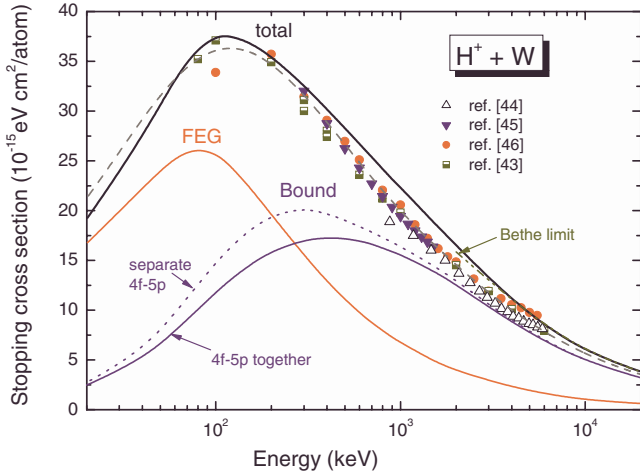
FIG. 2. (Color online) Stopping cross sections of W for protons. Curves: Solid lines present theoretical results for the contributions by bound electrons (SLPA) and the FEG and total stopping as the addition of the previous two; dashed line, SRIM08 results [4]; dotted lines, results obtained using the SLPA with independent $5p$ and $4f$ responses; dash-double-dotted line, Bethe high-energy limit given by Eqs. (2) and (3) with $I=727$ eV [29]. Symbols: experimental data [43–46].

FIG. 3. (Color online) Lindhard scaling for the stopping number. Symbols: theoretical SLPA results for W (filled stars), Au (filled circles), Pb (filled triangles), and Bi (hollow squares). Curves: dashed line, SRIM08 values for W; solid lines, Bethe limit as given by Eq. (3) for W ($I=727$ eV), Au ($I=790$ eV), and Pb ($I=823$ eV), with the mean excitation energies suggested by the ICRU Report 49 [29].

experimental data for the outer subshells of solid W (i.e., for the $4f\pm$, the GRASP values are 30% over the experimental ones). It should be noted that the binding energies are very sensitive to the atomic description but the differences in the radial wave functions were not so important.

Based on this study, we considered the HULLAC results the most reliable ones for W and employ them in the stopping and straggling calculations. The wave functions of wolframium are introduced in the SLPA in the form of multiple-Slater functions. To that end, a fitting procedure was performed.

III. ENERGY LOSS CALCULATION WITH THE SLPA

The SLPA is based on the original LPA by Lindhard and Scharff [18] and later on developments [19–23], but introduces two important differences: the independent shell approximation and the inclusion of the ionization thresholds. Physically, the independent shell approximation implies that the electrons are screened only by those of the same binding energy and not by the rest. Mathematically, it is a separate dielectric function of each subshell of bound electrons. The explicit inclusion of the binding energies is achieved by using the Levine-Louie dielectric response [26]. This dielectric function maintains the characteristics of Lindhard one [37] (linear response, electron-electron correlation) and satisfies the f-sum rule (particle number conservation).

In multielectronic targets such as W, we deal with subshells that are very close in energy. As mentioned before, we describe together those electrons with nearly equal binding energy, allowing screening among them. We consider together shells differing in ΔE_i small compared to the inverse of the passing time

with E_i and $\langle r \rangle_i$ being the energies and mean radius displayed in Table I.

Using this criterion, we have found that, for very heavy targets, the spin-orbit split $nl\pm$ is not resolved in most of the subshells. Moreover, in W, the $5p$ and $4f$ subshells are very close in energy and for impact velocity $v > 1$ a.u., the quantum uncertainty is bigger than the separation between them. This implies that the 20 electrons of the subshells $4f$ and $5p$ should be described as a whole including screening among them.

More details about the SLPA and the expressions for the stopping cross sections S and the square straggling Ω^2 can be found in previous works [12,25]. The stopping cross section can be expressed in terms of the dimensionless stopping number L as

$$S(v) = \frac{4\pi Z_P^2 Z_T}{v^2} L(v). \tag{2}$$

In the high-but-nonrelativistic velocity regime, the stopping number is described by the Bethe asymptotic formula [38]

$$\lim_{v \to \infty} L(v) = L^{\text{Bethe}}(v) = \ln\left(\frac{2v^2}{I}\right), \tag{3}$$

with I being the mean excitation energy, characteristic of the target material. It can be obtained basically in three different ways [39]: using the oscillator-strength data from measurements of photoabsortion cross sections, from measurements of stopping cross sections at high speeds, or in *ab initio* theoretical calculations. In this work, we use our theoretical stopping results at high energies to obtain the I values and

$$\Delta E_i \geq \frac{1}{\Delta t_i} = \frac{v}{\langle r \rangle_i}, \tag{1}$$

TABLE II. Mean excitation energies (in eV) for W, Au, Pb, and Bi. I^{SLPA} are present calculations using the SLPA; I^{ICRU} are the suggested values by the ICRU Report 49 [29]. Values used in other tabulations are I^B [48], I^J [49], and I^S [50].

	Z	I^{SLPA}	I^{ICRU}	I^B	I^J	I^S
W	74	710	727 ± 30	779	753	
Au	79	814	790 ± 30	788	807	799 y 810
Pb	82	810	823 ± 30	779	819	836 y 856
Bi	83	840	823 ± 30	745	819	

we analyze the tendency of the SLPA to Bethe high-energy limit.

IV. STOPPING AND STRAGGLING RESULTS

The *ab initio* calculations described in the previous section correspond only to the bound-electron contribution to the stopping or the straggling cross sections. In order to compare to experimental measurements, we also calculate the FEG contribution in perturbative approximation by employing the dielectric formalism with the Mermin-Lindhard dielectric function [40]. Total values are obtained as the addition of the bound electron and the FEG contributions.

The FEG parameters for W were obtained from the optical data of energy-loss function [41] by considering only the first important peak. Special care was taken of the number of electrons described. These values are a plasmon frequency $\omega_p = 0.894$ a.u., a width $\gamma = 0.450$ a.u., and the number of FEG electrons $Ne = 6.78$. These values are in good agreement with previous ω_p and Ne tabulated by Isaacson [42]. To keep the total number of electrons in the atom, we considered W in the form [Xe] $4f^{13.22}$ and the 6.78 electrons in the FEG.

In Fig. 2, we plot our total stopping cross section for protons in W and compare it to the experimental data available [43–46] and with the SRIM08 values. The FEG and bound-electron contributions are also displayed separately.

As mentioned in the previous section, $5p$ and $4f$ subshells of W, which are very close in energy, are described together. This means that intershell screening is included. In Fig. 2, we plotted in solid lines our results with the $4f$-$5p$ subshells as a whole (with 19.22 electrons), while in the dotted lines the six electrons $5p$ and 13.22 electrons $4f$ are considered independently (no intershell screening) and the contributions are added afterwards. The difference between solid and dotted curves is associated with the collective response and cannot be described by adding independent electron contributions. This is an important result of this work because it shows the importance of shielding among electrons, even from different subshells. The $5p$ and $4f$ subshells play an important role around the stopping maximum. But for energies above 1 MeV, both solid and dotted curves tend to the same limit. At very high impact velocities, the dynamic screening turns to be negligible and it is the same to consider the subshells together or not (SLPA or LPA).

Our total results describe rather well the experiments around the maximum and for very high energies, but overestimate the data in the region of a few MeV (i.e., they are

10%–14% above SRIM08 for $E = 0.7–3$ MeV). The SLPA predicts a maximum for the stopping cross section at $E = 115$ keV while SRIM08 does at $E = 120$ keV. In Fig. 2 we also include the Bethe high-energy limit for $E \geq 2$ MeV using the value of mean excitation energy $I(W) = 727$ eV suggested by the ICRU 49 reports [29]. The SLPA results tend to Bethe stopping for high energies, being both curves almost indistinguishable for $E > 3$ MeV.

To analyze with more detail the SLPA asymptotic behavior, we calculate the stopping number defined by Eq. (2). Many years ago, Lindhard and Scharff, based on dimensional reasons, proposed a scaling for L with v^2/Z_T valid for all elements of not too low atomic number [30]. In Fig. 3, we display the SLPA values for the stopping numbers of W, Au, Pb, and Bi (the latest three elements by employing the results of Ref. [12]). As shown in Fig. 3, the SLPA satisfies the scaling quite well.

We also display in this figure the Bethe stopping number given by Eqs. (2) and (3). The straight line in Fig. 3 is the overlapping of three straight lines obtained using the suggested mean excitation energies I for W, Au, and Pb in the ICRU 49 reports [29] (for Bi, the suggested value is interpolated from others and is equal to that of Pb [29]). As predicted by Bethe-Bloch theory $I = K Z_T$, where K is Bloch constant [47]. For these heavy targets $K = 10 \pm 0.2$ eV [29], so the three lines almost coincide.

The experimental data of stopping number for W, Au, Pb, and Bi also satisfy Lindhard-Scharff scaling rather well. We include in Fig. 3 the SRIM08 fitting [4] of the experimental data only for W just for simplicity. We can see how the SLPA is close to the SRIM08 curve at low and intermediate energies and that the high-energy behavior of the SLPA is related to tendency of this model to the Bethe limit.

The tendency of the stopping number to a straight line in a semilogarithmic plot of v^2 is fulfilled by the SLPA, but not by the experimental values. The theoretical-experimental difference observed in Fig. 3 in the energy region of 2–20 MeV may be related to complex physical mechanisms considered neither in the SLPA nor in Bethe formalisms. We obtained theoretical mean excitation energies I^{SLPA} for W, Au, Pb, and Bi. The results are displayed in Table II together with the experimental values [29,48–50]. The agreement is more than the expected one in the four elements, i.e., it is less than 3% with respect to the recommended I by the ICRU Report [29].

In Fig. 4, the SLPA results for the square of the energy-loss straggling are displayed normalized to the Bohr high-energy limit $\Omega_B^2/Z_T = 4\pi Z_P^2 \delta_{at}$, with δ_{at} being the target atomic density. This way of plotting the theoretical results
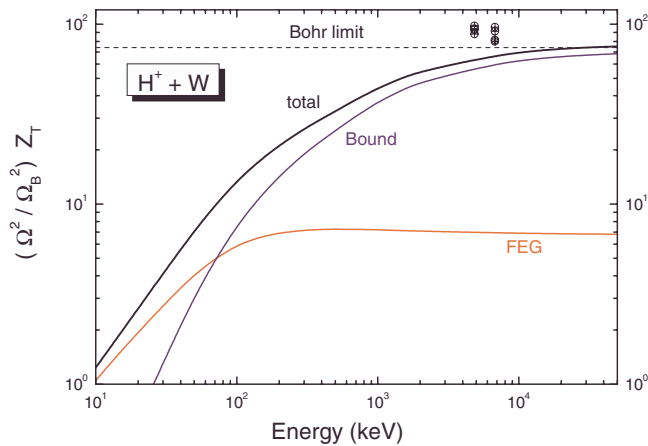
FIG. 4. (Color online) Square straggling of protons in W normalized with Bohr value over Z_T. Curves: present theoretical calculations. Symbols: experimental data by Bauer *et al.* [52].

stresses the high-energy tendency of the square straggling proportional to the number of active electrons, valid not only for the total value but for the separate contributions of the FEG and bound electrons too. Similar behavior for the energy-loss straggling was obtained in previous works [12,51] with good agreement with the experimental data.

To our knowledge, only one set of measurements of straggling of protons in W by Bauer *et al.* [52] has been published. These data are 30% over the Bohr limit, even though the impinging energies are rather high (4.9 and 6.8 MeV). These experimental energies are far from the energy region around the stopping maximum where the Bethe-Livingston shoulder [53] can explain this overshooting. These energies are also out of the region where the contribution of inhomogeneity and roughness of the sample could be important [54]. More measurements for this collisional system would be desirable.

V. CONCLUDING REMARKS

We present a theoretical study of energy loss and straggling of wolframium for protons. An *ab initio* many-electron formalism, the SLPA, is applied together with fully relativistic calculations of the atomic wave functions and binding energies. The HULLAC code was employed to obtain numerical solutions of the Dirac equation after being contrasted to other relativistic and semirelativistic methods. The role of the $4f$ and $5p$ subshells of W was especially studied and the electrons of these subshells are considered together, including the screening among all of them. Results for total stopping cross sections of protons in W are in rather good agreement with the experimental data for impact energies around the maximum and for high energies, but overestimate the measurements for energies of a few MeV. We found that the high-energy behavior of the SLPA is closely related to that of the Bethe asymptotic stopping. The SLPA stopping number for W, Au, Pb, and Bi follows the scaling with v^2/Z_T and tends to Bethe value for $E > 2$ MeV. Theoretical values for the mean excitation energies of the four elements have been calculated with very good agreement with the experimental values. Our straggling results are compared to the only set of data available at just two proton energies. In this case, more measurements are needed to have a clearer picture.

[1] H. Paul, Nucl. Instrum. Methods Phys. Res. B **261**, 1176 (2007).

[2] International Commission on Radiation Units and Measurements (I. C. R. U.) Report No. 73 (Oxford University Press, Oxford, 2005).

[3] P. Sigmund, *Particle Penetration and Radiation Effects*, Springer Series in Solid-State Physics 151 (Springer-Verlag, Berlin, 2006).

[4] J. F. Ziegler, http://www.srim.org

[5] H. Paul, Stopping Power for Light Ions: Graphs, Data, Comments and Programs in http://www.exphys.uni-linz.ac.at/stopping/

[6] P. M. Echenique, F. Flores, and R. H. Ritchie, Solid State Phys. **43**, 229 (1990), and references therein.

[7] A. F. Lifschitz and N. R. Arista, Phys. Rev. A **57**, 200 (1998).

[8] A. Salin, A. Arnau, P. M. Echenique, and E. Zaremba, Phys. Rev. B **59**, 2537 (1999).

[9] P. L. Grande and G. Schiwietz, in *Advances in Quantum Chemistry*, edited by J. Sabin (Elsevier, New York, 2004), Vol. 45, p. 7.

[10] P. Sigmund and A. Schinner, Eur. Phys. J. D **12**, 425 (2000).

[11] S. Heredia-Avalos, J. C. Moreno-Marín, I. Abril, and R. Garcia-Molina, Nucl. Instrum. Methods Phys. Res. B **230**, 118 (2005).

[12] C. C. Montanari, C. D. Archubi, D. Mitnik, and J. E. Miraglia, Phys. Rev. A **79**, 032903 (2009).

[13] P. Goya and P. Román, *Wolfram vs Tungsten*, Chemistry International 27 (International Union of Pure and Applied Chemistry IUPAC, Boston, 2005), No. 4, p. 26.

[14] M. Seki, Nucl. Fusion **47**, S489 (2007).

[15] R. D. Stambaugh, Proceedings of the 21st IAEA Conference (IAEA), p. IT/1–2.

[16] J. Schweinzer, *20th International Symposium on Ion-Atom Collisions*, p. 13 (unpublished).

[17] N. Baluc *et al.*, Nucl. Fusion **47**, S696 (2007).

[18] J. Lindhard and M. Scharff, Mat. Fys. Medd. K. Dan. Vidensk. Selsk. **27**, 1 (1953).

[19] E. Bonderup, Mat. Fys. Medd. K. Dan. Vidensk. Selsk. **35**, 1

(1967).

[20] W. K. Chu and D. Powers, Phys. Lett. **40A**, 23 (1972).

[21] C. M. Kwei, T. L. Lin, and C. J. Tung, J. Phys. B **21**, 2901 (1988).

[22] Y. N. Wang and T. C. Ma, Phys. Rev. A **50**, 3192 (1994).

[23] J. D. Fuhr, V. H. Ponce, F. J. García de Abajo, and P. M. Echenique, Phys. Rev. B **57**, 9329 (1998).

[24] C. D. Archubi, C. C. Montanari, and J. E. Miraglia, J. Phys. B **40**, 943 (2007).

[25] C. C. Montanari, J. E. Miraglia, M. Behar, P. F. Duarte, N. R. Arista, J. C. Eckardt, and G. H. Lantschner, Phys. Rev. A **77**, 042901 (2008).

[26] Z. H. Levine and S. G. Louie, Phys. Rev. B **25**, 6310 (1982).

[27] J. Oreg, W. H. Goldstein, M. Klapisch, and A. Bar-Shalom, Phys. Rev. A **44**, 1750 (1991).

[28] A. Bar-Shalom, M. Klapisch, and J. Oreg, J. Quant. Spectrosc. Radiat. Transf. **71**, 169 (2001).

[29] International Commission on Radiation Units and Measurements (I. C. R. U.) Report No. 49 (Bethesda, MD, 1993).

[30] J. Lindhard and M. Scharff, Phys. Rev. **85**, 1058 (1952).

[31] M. Klapisch, J. L. Schwob, B. S. Frankel, and J. Oreg, J. Opt. Soc. Am. **67**, 148 (1977).

[32] G. P. Williams, *Electron Binding Energies of the Elements*, CRC Handbook of Chemistry and Physics F170 (CRC Press, Boca Raton, 1986); *Electron Binding Energies*, X-Ray Data Booklet (Lawrence Berkeley National Laboratory, University of California, Berkeley, 1986), Chap. 2.2; in the web, an updated version can be found at http://www.jlab.org/gwyn/ebindene.html

[33] N. R. Badnell and M. S. Pindzola, Phys. Rev. A **39**, 1685 (1989).

[34] N. R. Badnell, J. Phys. B **30**, 1 (1997).

[35] I. P. Grant, B. J. McKenzie, P. H. Norrington, D. F. Mayers, and N. C. Pyper, Comput. Phys. Commun. **21**, 207 (1980).

[36] B. J. McKenzie, I. P. Grant, B. J. McKenzie, and P. H. Norrington, Comput. Phys. Commun. **21**, 233 (1980).

[37] J. Lindhard, Mat. Fys. Medd. K. Dan. Vidensk. Selsk. **28**, 1 (1954).

[38] A. Bethe, Ann. Phys. (Leipzig) **5**, 325 (1930).

[39] S. Kamakura, N. Sakamoto, H. Ogawa, H. Tsuchida, and M. Inokuti, J. Appl. Phys. **100**, 064905 (2006).

[40] N. D. Mermin, Phys. Rev. B **1**, 2362 (1970).

[41] *The Electronic Handbook of Optical Constants of Solids*, edited by E. D. Palik and G. Ghosh (Academic, San Diego, CA, 1999).

[42] D. Isaacson, New York University Doc. No. 02698 (National Auxiliary, New York, 1975).

[43] E. I. Sirotinin, A. F. Tulinov, V. A. Khodyrev, and V. N. Mizgulin, Nucl. Instrum. Methods Phys. Res. B **4**, 337 (1984).

[44] E. I. Sirotinin, A. F. Tulinov, A. Fiderkevich, and K. S. Shyshkin, Radiat. Eff. Defects Solids **15**, 149 (1972).

[45] M. Luomajarvi, Radiat. Eff. Defects Solids **40**, 173 (1979).

[46] V. Ya. Chumanov, Sh. Z. Izmailov, G. P. Pokhil, E. I. Sirotinin, and A. F. Tulinov, Phys. Status Solidi A **53**, 51 (1979).

[47] W. Brandt, Phys. Rev. **104**, 691 (1956).

[48] H. Bichsel, Phys. Rev. A **46**, 5761 (1992).

[49] J. F. Janni, At. Data Nucl. Data Tables **27**, 147 (1982).

[50] N. Sakamoto *et al.*, Radiat. Eff. Defects Solids **117**, 193 (1991).

[51] C. C. Montanari, J. E. Miraglia, S. Heredia-Avalos, R. Garcia-Molina, and I. Abril, Phys. Rev. A **75**, 022903 (2007).

[52] G. H. Bauer, A. J. Antolak, A. E. Pontau, D. H. Morse, D. W. Heikkinen, and I. D. Proctor, Nucl. Instrum. Methods Phys. Res. B **43**, 497 (1989).

[53] M. S. Livingston and H. A. Bethe, Rev. Mod. Phys. **9**, 245 (1937).

[54] J. C. Eckardt and G. H. Lantschner, Thin Solid Films **249**, 11 (1994).